A large insertion in intron 2 of the TYRP1 gene associated with **American Palomino** phenotype in American mink

Mamm Genome
DOI 10.1007/s00335-016-9620-4

A large insertion in intron 2 of the *TYRP1* gene associated with *American Palomino* phenotype in American mink

Susanna Cirera[1] · Marios Nektarios Markakis[1,2] · Thea Kristiansen[1] · Kris Vissenberg[2] · Merete Fredholm[1] · Knud Christensen[1] · Razvan Anistoroaei[1]

Received: 4 December 2015 / Accepted: 31 January 2016

Abstract A number of American mink phenotypes display a range of brownish colours. One of these phenotypes, namely *American Palomino* (b^Pb^P) (*AP*) has been found to be associated with the *tyrosinase-related protein 1 (TYRP1)* gene by genotyping microsatellite markers in one sire family. Trials for amplifying the genomic DNA and cDNA at the beginning of intron 2 of *AP TYRP1* revealed the presence of a large insertion of approximately eight kb. The insertion most likely disrupts different elements necessary for the splicing of intron 2 of the *TYRP1* gene. In *AP* RNAseq data indicate, however, the presence of the wild-type (*wt*) transcript at very low levels and Western blot reveals three products when using an antibody raised against middle part of the TYRP1 protein. One individual from another brown mink phenotype—commercially named *Dawn*—was also investigated at the molecular level by long-range PCR and the same size insertion appears to be present. By this we suggest that certain modifiers of TYRP1 would induce different brown colour degradation, which results in at least two different phases of brown.

Electronic supplementary material The online version of this article (doi:10.1007/s00335-016-9620-4) contains supplementary material, which is available to authorized users.

✉ Razvan Anistoroaei
ran@sund.ku.dk

Susanna Cirera
scs@sund.ku.dk

[1] Department of Veterinary Clinical and Animal Sciences, Section of Genetics, Bioinformatics and Animal Breeding, Faculty of Health and Medical Sciences, University of Copenhagen, Groennegaardsvej 3, 1870 Frederiksberg C, Denmark

[2] Department of Biology, Integrated Molecular Plant Physiology Research, University of Antwerp, 2020 Antwerp, Belgium

Introduction

In American mink (*Neovison vison*), a total of 12 phenotypes display a brown appearance in a wide range (Nes et al. 1988; Fig. S1). However, the farming and commercial names of these colours are not based on a very clear phenotype description but rather on a specific grading. The latter is set at the fur centres where a certain phase is graded by experts and/or machines and allocated to a commercial name. All brown phenotypes are inherited as a simple recessive trait, thus only homozygous individuals display the phenotype. The various brown coat colours in American mink have a brownish appearance that can vary within the phenotype but also during the animal life. However, for commercial purposes the colours are recorded at the pelting time, which is when the fur colour has reached its "maturity". One important colour in the brown spectrum of mink is *American Palomino* (*AP*) (Fig. S2.A) symbolized as *kk* in the Scandinavian nomenclature and b^pb^p in the American nomenclature (Nes et al. 1988). The *AP* mutant appeared first in a farm in Canada in the middle of the twentieth century (King 1951). The coat colour appears as a clear pale tan, and on a prime pelt it easily turns slightly red while the eyes are pink or red (Nes et al. 1988). Currently, only few pure *AP* mink are commercially produced as the colour is used particularly in combination with genes encoding grey colour such as the *Aleutian* colour gene (b^pb^pll) (Anistoroaei et al. 2012) and the *Silverblue* dilution gene (b^pb^pdd) (Cirera et al. 2013). It is also segregating in back-crosses of the *AP* phenotype (b^Pb^Ppp).

Published online: 17 February 2016

Another brown phenotype, which has a darker appearance than the *AP*, is commercially called *Dawn*.

In American mink, Shackelford (1980) described for the first time that different mutations of the *b* locus, alone or in combination with other loci bring different brown colour phases such as Green-eyed pastel (*bgbg*), Moyle buff (*bmbm*), Ambergold (*abab*) and Socklot (*bsbs*). In several species, brownish phenotypes have been found to be associated with the *b* locus (*TYRP1*): in dog (Schmutz et al. 2002), pig (Ren et al. 2011), sheep (Gratten et al. 2007), cat (Schmidt-Küntzel et al. 2005; Lyons et al. 2005), cattle (Nonneman et al. 1996; Berryere et al. 2003; Mohanty et al. 2008), horse (Rieder et al. 2001) and Japanese quail (Nadeau et al. 2007) it has been reported that brown phenotypes are caused by specific mutations in the *TYRP1* gene. Moreover, a small number of mutations in the *TYRP1* gene have been found to cause oculocutaneous albinism type 3 in humans (Kenny et al. 2012).

Tyrosinase-related protein-l (also known as *5,6-dihydroxyindole-2-carboxylic acid oxidase*, *DHICA, TYRP1*) was named as such due to its homology to tyrosinase (Jackson 1988). It is one of the three tyrosinase-related protein (TRP) family members, besides *Tyrosinase* (*TYR*) and *Dopachrome Tautomerase* (*Dct*). These three enzymes are type I membrane glycoproteins with significant structural homology, and they are all targeted to and located in the melanosomal membrane. They are part of a cascade reaction in the melanogenic pathway controlling melanin production in melanosomes (Hearing 1999, 2005; Wang and Hebert 2006). TYRP1 is one of the most abundant glycoproteins in melanocytic cells (as reviewed by Kobayashi and Hearing 2007), and it thus plays an intrinsic role in the formation and stabilization of melanogenic enzyme complexes. While TYR product abnormalities lead to oculocutaneous albinism, also described in mink (Anistoroaei et al. 2008; Benkel et al. 2009), TYRP1 has distinct catalytic functions in melanin synthesis downstream of TYR. In contrast to mutations in *TYR*, mutations in *TYRP1* affect the quality of synthetized melanin rather than the quantity (Kobayashi and Hearing 2007). In brown mouse, the melanin produced by a mutant *TYRP1* gene is less polymerized compared to the melanin in wild-type (*wt*) mice (Ozeki et al. 1995). TYRP1, in addition to having enzymatic functions, stabilizes TYR and co-expression of TYR with TYRP1 in melanocytes, which increases pigmentation (as reviewed by Kobayashi and Hearing 2007). Moreover, TYRP1 determines whether eumelanic pigment will be black (when active) or brown (when inactive or absent) (Bennett et al. 1990; Zdarsky et al. 1990). In mink, like in other species, brown types produce only slightly less eumelanin than *wt* mink (Figs. S1, S2). The *TYRP1* gene is represented by 7 exons with a full-length coding sequence of 1.6 kb, yielding a protein of 537 amino acids, including the signal peptide (Sturm et al. 1995). The mature glycosylated protein has a molecular weight of about 75 kDa (Halaban and Moellmann 1990; Hearing and Tsukamoto 1991).

In this study, we have mapped the locus responsible for one of the mink brown phenotypes—*AP*—to be *TYRP1* gene. Comparisons of the *TYRP1* genomic DNA sequences between *wt* and the *AP* mink, revealed a large insert at the beginning of intron 2. The insert was also detected in a *Dawn* phenotype by long-range PCR. This is the first reported case of a b-locus mutation caused by an enlarged intronic insertion in the animal world. Our results lead us to hypothesize that this large insertion prevents the splicing machinery from removing intron 2 containing the insertion, which results in a disrupted splicing model. RNAseq data indicate that the normal transcript with intron 2 spliced out is also found but at significantly much lower levels when compared to the abundance of the transcript retaining intron 2 with the insertion or skipping the exon 2. This finding is also supported by results provided by Western blot, when an antibody raised against the middle part of the TYRP1 protein was used.

These findings enable the development of genetic tests for analyzing the colour selection in American mink and supplement the catalogue of brown colours in mammal species involving the TYRP1 protein.

Materials and methods

Family material, markers and genotyping

From the existing literature, one of the obvious candidate genes for brown phenotypes is the *TYRP1* gene representing the b-locus. We therefore aimed at developing microsatellite markers from the region where this gene is located. *SOAP*-assembled (Luo et al. 2012) 100-bp end reads from next generation sequencing (NGS) data from a *wt* mink were aligned against the ferret genomic assembly (*MusPutFur* 1.0) and subsequently used to assemble the *TYRP1* gene sequence in mink. A part of the contig located 1.3 Mb upstream from the *TYRP1* gene contained microsatellite repeat elements allowing us to develop two microsatellite markers—*TYRP1m1* and *TYRP1m2* (Table S1)—which were used for genotyping.

One sire family with four litters originating from a Danish farm in Zealand having 15 informative offspring that segregated for the *AP* colour (Fig. S3) and which was earlier used in the first linkage study for the American mink (Anistoroaei et al. 2007) was genotyped with the two microsatellite markers for the b-locus. DNA isolation was performed as described in Anistoroaei et al. (2007). Two additional DNA samples from random *AP* mink originating

from a farm in Fyn, Denmark were isolated from clipped nails using the 5 % Chelex 100 (Bio-Rad) solution following the recommended protocol (Walsh et al. 1991). Genotyping on the mink *AP* family was performed with fluorescently labeled forward primers (HEX and NED, respectively) on an ABI Prism 3130 sequencer, and genotypes were analyzed using GenScan analysis (v.3.1.2) software (Applied Biosystems).

In addition, a sample from *Dawn* phenotype was obtained from a Danish farm and DNA was extracted from spleen and from nail, using the above-mentioned protocols. Segregating family material for this phenotype was, however, not available. Therefore the further investigation was only made at the DNA level for one individual.

For the design of the primers for all purposes (markers, genomic DNA, cDNA), Primer3 software (http://frodo.wi.mit.edu/cgi-bin/primer3/primer3_www.cgi) was used.

Primers for each exon of the *TYRP1* gene were designed from the flanking intronic regions (Table S2). DNA fragments spanning the exon sequences of the *TYRP1* gene were amplified by PCR and sequenced. Sequencing was performed using BigDye Terminator Cycle Sequencing chemistry (Applied Biosystems) following the manufacturer's recommendations, and the resulting purified products were separated on an ABI 3130 Automated Nucleic Acid Analyzer. DNA sequences were processed using Lasergene (DNA Star Inc.). Sequence differences were identified by comparing brown individuals with *wt* sequence using BLAST *bl2seq* at NCBI.

RNA isolation

Total RNA was isolated from two tissues for different experiments: retina from *AP* mink to be used for NGS on the Illumina™ 2000 platform and from kidney from *AP* and *wt* mink to be used for cDNA amplification by PCR. Retina was used for RNAseq due to the high abundance of TYRP1 expression in this tissue (http://www.genecards.org/cgi-bin/carddisp.pl?gene=TYRP1).

RNA from kidney was isolated using RNeasy mini kit (Qiagen, Germany) following manufacturer's instructions. Briefly, approximately 20 mg of tissue was homogenized in two ml of RLT® buffer containing beta-mercaptoethanol using gentleMACS™ Octo Dissociator (Miltenyi Biotec), as recommended by the manufacturer. A DNAse treatment step was also performed in the protocol to degrade possible remaining genomic DNA. RNA from one entire retina was isolated using TRI Reagent® protocol and gentleMACS™ Octo Dissociator (Miltenyi Biotec) as recommended by the manufacturer. The genomic DNA was removed from the sample using the Clean-up kit (Qiagen, Germany). For all samples, RNA concentration and purity were assessed in a NanoDrop instrument (Thermo Scientific). The RNA quality of the samples was visually inspected by gel electrophoresis and the integrity was further assessed on a BIO-RAD Experion™ engine using the Experion™ RNA StdSens analysis kit to obtain RQI number. RQI values for all samples were >8, confirming a very good quality of the RNA.

cDNA synthesis

One µg of total RNA DNAse-treated from kidney of *AP* and *wt* animals, respectively, was used for cDNA synthesis using ImProm-II reverse transcriptase (Promega) and a 3:1 mixture of random hexamers/Oligo(dT) Primers, according to the manufacturer's instructions. cDNA was diluted eight times before being used for PCR.

NGS and data processing

DNAseq of American Palomino and Wild Type mink

Two DNA samples, one originating from an *AP* and one from a *wt* mink (the same *wt* individual utilized in the construction of an American mink BAC library (Anistoroaei et al. 2011)) were commercially sequenced using the Illumina™ platform (AROS Applied Biotechnologies, Denmark). The samples were 100 bp pair-end sequenced in one lane of an Illumina™ HiSeq 2000 sequencer. Sequence data were *de novo* assembled by SOAP (Luo et al. 2012), and the resulting contigs were aligned to the ferret (*Mustela putorius*) b-locus (NW_004569257.1 from 5623237 to 5659924) using BLAST (Altschul et al. 1990).

RNAseq of retina sample from *AP* mink

Prior to library preparation, the RNA quality and integrity was assessed according to Illumina™ guidelines. Library preparation was done using the TruSeq® Stranded mRNA sample preparation 96 rxn kit (Illumina™) following the low sample protocol according to manufacturer's recommendations. Subsequently, the library was quantified using PicoGreen® dye (Life Technologies™) as described in the manufacturer's protocol. In order to accurately quantify the concentration in nM of the sample, the KAPA SYBR® FAST universal qPCR kit (Kapa Biosystems™) for Illumina™ sequencing was used to quantify the number of the amplifiable molecules in the sample, and the Bioanalyzer® machine (Agilent Technologies™) was used to determine the average fragment size of the sample. These measurements allowed optimizing the flow cell clustering and the proceeding with the Run. The sample was 50 bp pair-end sequenced in one lane of an Illumina™ HiSeq 2000 sequencer.

Resulting sequence data were assembled by Velvet 1.2.07 (Zerbino and Birney 2008) and aligned to the ferret (*Mustela putorius*) b-locus (NW_004569257.1 from 5623237 to 5659924) by BLASTN (Altschul et al. 1990). For quantifying the expression level of each exon and the expression level of the exon–exon passage using the paired ends reads, bowtie (Langmead and Salzberg 2012) software was employed.

In order to accurately expand over sequence gaps making use of the pair-ends from the NGS, the reads were aligned by means of bowtie (Langmead and Salzberg 2012) with the default options.

Long range PCR

Genomic DNA from the different brown phenotypes, namely *AP, Dawn* and *from wt* was used to perform a long-range PCR using PrimeSTAR® GXL DNA Polymerase (Takara Bio INC, France) with two primer combinations: (1) forward primer at the end of exon 2 and reverse primer at the beginning of exon 3 and; (2) forward primer at the end of exon 2 and reverse primer designed immediately after the inserted sequence (Table S3). Conditions were optimized to use 500 ng of genomic DNA and 8 min extension time in a total volume of 50 µl. The second primer combination was used to sequence the 3́end of this 8 kb PCR product in *AP* and *Dawn* phenotypes, respectively. The PCR products were isolated from a gel, and DNA was purified using the Illustra™ GFX™ PCR DNA and gel band purification kit (GE Healthcare, UK) according to the manufacturer's protocol. Fifty ng of PCR-cleaned product was sequenced using a primer located in intron 2 and BigDye Terminator Cycle Sequencing kit (Applied Biosystems) following the manufacturer's recommendations. The resulting purified products were separated on an ABI 3130 Automated Nucleic Acid Analyzer. DNA sequences were processed using Lasergene (DNA Star Inc.). Sequences were compared using BLAST *bl2seq* at NCBI.

Protein isolation and Western blot

Proteins were isolated from 20 mg of kidney tissue from a *wt* and from *AP* mink, respectively. Moreover, proteins were also isolated from 20 mg of pig pancreas to be used as a positive control. Proteins were isolated using the AllPrep® DNA/RNA/Protein purification kit (Qiagen, Germany) following manufacturer's recommendations, except for the last step where the protein pellet was dissolved in 5 % SDS. Proteins were quantified in a NanoDrop instrument (Thermo Scientific). Subsequently, 40 µg of protein, LDS sample buffer and sample reducing agent were mixed for each sample prior to loading on a 7 % Tris–Acetate gel (Life Technologies). Proteins were separated at 100 volts for 1.5 h. Following electrophoresis, the proteins were transferred to a PVDF membrane using an Invitrogen transfer system (Invitrogen, Life Technologies, Carlsbad CA, USA) according to the manufacturer's instructions except that the voltage was raised to 130 V and the time was extended to 1.5 h to ensure sufficient transfer. Subsequently, the membrane was stained with Ponceau S Staining Solution (Sigma-Aldrich) to asses successful transfer of the proteins to the membrane and afterwards, the stain was removed by washing with 0,1 M NaOH. The WesternBreeze Chemiluminescent Western Blot Immunodetection kit (Invitrogen, Life Technologies, Carlsbad CA USA) was used following manufacturer's instructions, except that the blocking time was extended to overnight. The primary antibody used was raised against the synthetic peptide TYRP1 human AA residues 340-371 (encompassing part of exon 4 and exon 5) (antibody provided by Nordic BioSite, LS-C157304). The sequence encompassed by the antibody was 100 % conserved between human, pig and mink. The Primary antibody was diluted according to the manufacturer's instructions (1:1.000). The membrane was exposed for 40 min prior to developing the X-ray film.

Results

Identification of TYRP1 as the causative gene for *AP* phenotype

The genotyping of the two microsatellite markers (*TYRP1m1 and TYRP1m2*—Table S1) close to the *TYRP1* gene in the family segregating for the *AP* phenotype (Fig. S2.A) revealed informative polymorphism for both markers. The two markers yielded identical statistically significant results for the relationship with the *AP* phenotype: $\chi^2 = 8.75$ (df = 1; $p < 0.01$). Based on mink sequence homology to human and dog (Graphodatsky et al. 2000; Hameister et al. 1997), the gene and sequences were located to mink chromosome 2, close to the centromere.

Amplification of exons from genomic DNA

PCR amplification of individual exons of *TYRP1* was performed for *wt* and *AP,* respectively. Amplicons based on the initial primer design (Table S2) were only obtained for exons 1 and 3–7; thus further re-designing was performed in various combinations in an attempt to obtain an amplicon of exon 2. The various primer designs are not included in this report as it did not produce relevant information, other than the fact that the region at the end of exon 2 was un-amplifiable.

A comparison between the *wt* and *AP* nucleotide sequences of the amplified exons (1 and 3–7) and flanking regions of the *TYRP1* revealed no nucleotide differences between the phenotypes.

Amplification of the transcript from cDNA

Several combinations of primers encompassing the coding region of *TYRP1* were used. These combinations made it possible to amplify the following parts of the c*TYRP1*: c34-c956 (exons 1–4) and c525–c798 (exon 2–3) resulted in amplicons in *wt* but not in *AP,* while a combination of primer pairs between exons 3 and 7 (c747–c1589) resulted in amplicons from both phenotypes.

Processing of the NGS data

DNAseq of AP and wt mink and RNAseq of AP mink

The DNA from the *AP* mink sample yielded a total of 265.173.632 pair-end (100 bp) reads while the DNA from the *wt* sample yielded 285.196.308 pair-end (100 bp) reads. The RNA *AP* sample yielded a total of 70.245.702 pair-end reads (50 bp).

The search master sequence used for various alignments was the ferret b-locus NW_004569257.1 from 5623237 to 5659924. Sequences produced by SOAP assembly software for the genomic DNA from the *wt* mink and from the *AP* mink covered the master sequence with more than 95 %. A striking difference between the two assemblies occurred between exon 2 and exon 3.

For the *wt* mink, the region spanning the end of exon 2, intron 2 and beginning of exon 3 resulted in the expected sequence contig and no elements of the insert were captured in the region. The assembled mink *TYRP1* gene has been deposited at NCBI (#KU186800).

Investigation of the *AP* mink sequence for this region showed a similar repeat at each end. They were assembled by means of the hanging ends of the pair-ends using Bowtie software and subsequently verified by PCR and sequencing. These repeats consist of three distinct elements. The first element located immediately after exon 2, consists of 374 bp hereon called "Mustelid" which is also found in other regions of the mink genome and matches to only one sequence in *Mustela putorius* sequences when searched against the nucleotides database at NCBI. This is the only reason for which we consider the sequence to be "mustelid" and not "mink" specific. This first element is followed by a sequence of 218 bp having homology to a region in a retrovirus hereon called "Viral", sequence found ubiquitously integrated in the genome of many different species when searched in the NCBI nucleotide database. The third part consists of a short sequence of 56 bp which appears to be very unique as it does not align to any database sequence. The sequences at their insertion point are depicted in Fig. 1. The cassette has been deposited at NCBI database (#KU186801). Due to the fact that this sequence occurs relatively frequent within the mink genome, further extension of the region into the insert was impossible.

Identification of a large insertion in intron 2 of TYRP1 in *AP*, also confirmed in *Dawn* mink

We performed a long-range PCR in order to amplify the suspected insertion at the beginning of intron 2 in one animal from each of the brown phenotypes. In the *wt*, the PCR amplification of the fragment between the end of exon 2 and the beginning of exon 3 resulted in a product size of approximately 3 kb. In *AP* and *Dawn*, the amplified fragment was larger than 11 kb indicating the presence of a large insertion. When using the same forward primer together with a primer designed in intron 2 of the *wt* sequence (Table S3), we confirmed a PCR product of the expected size (110 bp) in the *wt* and a PCR product of around 8 kb in *AP* and *Dawn*. After sequencing the 3′ end of the 8 kb PCR product in these 2 phenotypes, we confirmed that the cassette with the three regions (mustelid/virus/unspecific sequence) is found at the end of the inserted fragment in *AP* and *Dawn*. Approximately 200 bp upstream, the cassette at the 3′end of the inserted sequence were also sequenced and appeared to be homologous to one unannotated genomic sequence from American mink (#DQ271520.1).

In order to verify whether this insert in intron 2 is also retained in the cDNA, possibly interfering in the splicing, we performed a PCR on cDNA from kidney of *AP* using a primer designed at the end of exon 2 and a primer located in the inserted sequence and we obtained a PCR product, which confirmed the retention.

The mink exons for the *TYRP1* gene have been derived from the assembled sequence of the *wt* mink. Using these exons as a bowtie master for the RNAseq data, we could extract the number of reads which hit two different exons (Table 1).

In addition, investigations of the different parts of the insert using the Bowtie application pointed out their presence throughout the mink transcriptome as presented in Table 2, column 2 . Thus, the mustelid-specific element occurs almost four times more frequently than the viral element while the presence of a connected sequence containing the mustelid specific and the viral element occurs in the transcriptome about five times more frequently than when connected to exon as shown in Table 1. Using the same protocol, we also performed investigations of the different parts of the insert using the Bowtie application throughout the mink genome with findings indicated in Table 2, column 3.

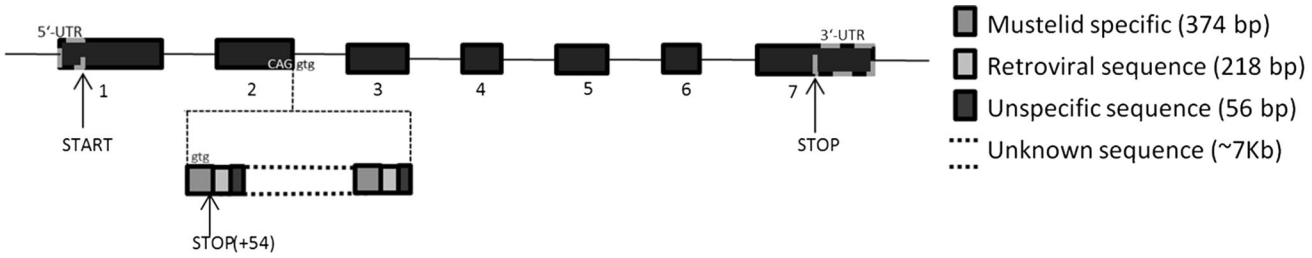

Fig. 1 Depiction of *TYRP1* gene in American mink with reference to the insertion found in the two brown phenotypes. Note that the splicing site is identical with or without the insert. A stop codon appears nevertheless 54 nucleotides downstream into the insert

Table 1 Exon splicing as detected from the NGS RNAseq data of one *AP* colour type

Exon	No. of reads encompassing the exons boundaries
1–2	539
2–3	1
3–4	29
4–5	24
5–6	19
6–7	22
1–3	7
3–7	1
2 to Mustelid	594

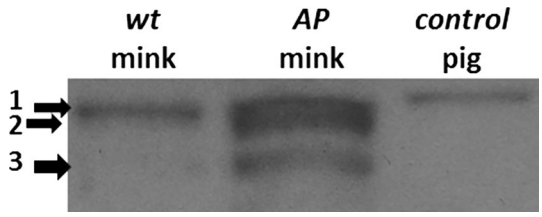

Fig. 2 Western blot of TYRP1. A band, representing the *wt* TYRP1, at approximately 75 kDa can be seen in the *wt* mink, in control pig but also in the *AP* mink. Additionally two shorter bands representing two shorter isoforms of this protein are seen in the *AP* mink

TYRP1 protein identification by Western blot

Western blot hybridization using an antibody from the region encompassing residues corresponding to exon 4–exon 5 revealed one isoform in *wt* mink and in pig of around 75 kDa, as expected (Fig. 2). In *AP* mink sample two very close bands appear at the *wt* size range, showing the full-length isoform and an isoform very close to be full-length, together with an isoform a bit shorter (in the range of 70 kDa) (Fig. 2). Based on the location of the antibody epitope (exon4–exon5), only two of the isoforms can be correlated to the splice forms found in our NGS data (Table 1), while the third isoform is assumed not to have been captured in the RNA seq data.

Discussion

Brown coat colour variations have been recognized in a variety of species and in American mink. In mink, there have been assigned several loci inducing brown colouration. The *wt* dark brown is the dominant type and is similar to the colour of original mink in the wild (Fig. S1). Other varieties of brown are recessive type, and they are commercially named in various ways according to the grading of brown obtained at the fur auction houses. Several alleles are assigned in brown-coloured mink, such as normal brown pigmentation of the *wt* (Fig. S1) or the brown phenotype corresponding to *AP* (b^P) (Fig S2.A).

The analysis of a pedigree segregating for *AP* confirmed that the phenotype is recessive to *wt*. However, no families for *Dawn* phenotype have been investigated. The linkage analyses supported *TYRP1* as the candidate gene for the *AP* phenotype. Based on mink sequence homology to human and dog (Graphodatsky et al. 2000; Hameister et al. 1997), the *TYRP1* gene is located on mink chromosome 2, close to the centromere.

The two brown phenotypes investigated at molecular level in the present study are consistent with an insertion of, approximately, 8 kb in intron 2. There is apparently no difference in size of the insertion between the *AP* and *Dawn* alleles, as derived from the long-range PCR analysis

Table 2 The occurrence of the mustelid and the viral elements, respectively, as retrieved from the NGS RNA data

Element	No. of reads allocated to the elements of the insert in the transcriptome	Approx. no. of reads allocated to the elements of the insert in the genome
Mustelid to Viral	2844	500
Mustelid to …	11.294	360
Viral to …	2843	500

encompassing the region of interest. Therefore, the two brown phenotypes have the same insertion suggesting that several brownish phenotypes are caused by the same insertion that is identical by descent across these three colour lines. Therefore, the brown colour might be modified by alleles (modifiers) in other coat colour loci. However, the implication of intron retention has been demonstrated in a large-scale analysis of human transcripts (Galante et al. 2004); thus, it cannot be ruled out that the retained intron event might have been under selection for coding potential and this in fact reflects biological significance. The retention of intron 2 containing the insertion in *AP* creates a premature stop codon at nucleotide 54 downstream of exon 2 (Fig. 1), which virtually results in a shorter protein that might be, but not necessarily is, non-functional. It is noteworthy that the acceptor and donor splice sites are still found in intron 2 (Fig. 1) which could explain the existence of rare normal transcripts in the RNA seq data. It is generally accepted that the splicing machinery is 'noisy' (e.g. Zhang et al. 2009) and in this case the machinery might very well be able to overcome the insertion in rare occasions. This theory supports the findings in our study where a very low number of *wt* transcripts have been identified in the RNAseq data from *AP*. The identified insertion in *AP* and *Dawn* American mink is not similar to any previously identified mutations in brown phenotypes of other species involving the *TYRP1* gene, and until now, no molecular description for brown recessive mutation (b) in Mustelidae has been reported. Mutations identified in other mammalian species all encompass the coding region of *TYRP1*: in pig a 6-bp deletion in the *TYRP1* gene (Ren et al. 2011) reduces the product with two amino acids; in dog, deletion of a proline residue in exon 5 (345delP) leads to a brown phenotype (Schmutz et al. 2002). Moreover, non-synonymous mutations resulting in amino acids substitutions in *TYRP1* appear to be the most frequently associated mutations with brown variants in various species. Namely, homozygosity for a H434Y amino acid substitution (exon 7) in cattle (Berryere et al. 2003); homozygosity for a C290F (exon 4) in sheep (Raadsma et al. 2013); a Phe282Ser (exon 4) in quail (Nadeau et al. 2007); a C189T (exon 2) in horse (Rieder et al. 2001) and a S41C (exon 2) in dog (Schmutz et al. 2002). Moreover, a premature stop codon due to nonsense mutation has been described in the dog—exon 5 (Q331X) (Schmutz et al. 2002) and Cinnamon cat—exon 2 (R100X) (Lyons et al. 2005). Besides animal species, two mutations in the *TYRP1* gene have been found to cause oculocutaneous albinism type 3 in humans: S166X and 368delA (Kenny et al. 2012).

The *TYRP1* variant in mink appears to be associated with different shades of brown, which is also true in the mouse and cat. However, the variations in pigment intensity can be caused by the environmental conditions, modifiers, dilution factors of other genes influencing pigmentation and minor polygenic effects. This makes it very challenging for breeders to distinguish the phenotype of brown present in mink. Thus, if adopted as genetic tests for colour, these mutations can improve the efficiency of breeding programs for a variety of colour lines.

Brown phenotypes are caused by mutations in the *TYRP1* gene resulting in defective production and storage of melanin pigments. TYRP1 is not expressed in cells that are producing pheomelanin (yellow background). As a result, a yellow pigmentary phenotype is epistatic to nonyellow (eumelanic)—black or brown. For this reason, there can be a slight variation in the appearance of the phenotypes of the brown animals that are homozygous for *TYRP1* (Brown) pointing out that other loci and/or environmental factors could be playing a role (Lamoreux et al. 2010).

The mink *TYRP1* gene contains seven exons, and the predicted transcript is 1611-bp long with an open reading frame translating into 537 amino acids (NCBI # KU186800). A BLAST comparison of mink and ferret (the closest relative to mink with available *TYRP1* gene sequence) for the *TYRP1* sequences revealed nucleotide and deduced amino acid sequence similarities of 99 and 98 %, respectively, whereas similarities between mink and dog were 93 and 94 %, respectively.

The TYRP1 protein is most likely involved in the stability of the tyrosinase enzyme (TYR), the most essential enzyme in the catabolism of the melanin. Kobayashi et al. (1994) showed that TYR degradation in TYRP1 mutant cells was significantly quicker than in TYRP1 *wt* cells. Furthermore, Toyofuku et al. (2001) demonstrated that mutant TYRP1 forms a complex with TYR in the ER of melanocytes, which results in the proteasomal degradation of *wt* TYR. Later, Kobayashi and Hearing (2007) demonstrated in vivo interaction between TYR and TYRP1 and they suggest that the N-terminal region of TYRP1 is critical for this interaction. Taken together, these studies demonstrate that TYRP1 interacts directly with TYR in melanocytes and probably also in melanosomes and thus determines pigment biosynthesis.

Our Western blot hybridization results indicate three isoforms specific to *AP* phenotype (Fig. 2). Two of the bands are presumed to correlate with the predicted isoforms derived from the RNAseq NGS data (Table 1), but they should be regarded as a qualitative result only. A third isoform was not captured in the assembled RNAseq data from the *AP*. In the context of the described role of TYRP1 (Kobayashi and Hearing 2007), it can be hypothesized that an insufficient amount of the full-length TYRP1 (see Table 1) and/or the presence of additional isoforms could lead to brown variations in the described phenotypes. A

provocation for future research regarding the brown loci in American mink would be to comparatively analyze the level of transcription for different *TYRP1* isoforms between various brown phenotypes, which might have the same insertion in intron 2 as described in this paper. One hypothesis is that random splicing at the end of exon 2, due to this insertion, might produce different levels of full-length *TYRP1,* which subsequently will induce the brown pigmentation in various grades. Another provocation would be the investigation and sequencing of most of the insert (between the two repeat elements), a task which could not be undertaken in this project due to a number of constrains.

In conclusion, we have mapped the locus responsible for the mink *AP* phenotype using specifically designed microsatellite markers developed close to the *TYRP1* gene contig. A large insertion in intron 2 is characteristic for two brown phenotypes in American mink, namely *AP* and *Dawn*. Amplification of cDNA from kidney of an *AP* mink demonstrates the retention of this insert in the transcript. Western blot analysis showed that full-length protein is still synthesized but, according to the NGS results, probably in an insufficient amount leading to brown variations in the described phenotypes. The identification of this mutation in the *TYRP1* gene provides the basis for establishing a DNA selection tool for American mink that are carriers of the recessive brown colour phenotypes.

Acknowledgments This work was supported from private funding. We are thankful to Tina B. Neergaard Mahler and Minna Jakobsen for technical assistance. We acknowledge Boye Pedersen who is in charge of the KU mink farm. We also acknowledge Jesper Clausen for providing some of the pictures of the mink.

Compliance with ethical standards

Conflict of interest The authors declare not having any conflict of interest. The authors are investigation scientists and although they work with a politically controversial fur animal species, herein they are only supporters of the science. Their political view might therefore differ from the line of research they are engaged in.

References

Altschul SF, Gish W, Miller W, Myers EW, Lipman DJ (1990) Basic local alignment search tool. J Mol Biol 215(3):403–410

Anistoroaei R, Menzorov A, Serov O, Farid A, Christensen K (2007) The first linkage map of the American mink (*Mustela vison*). Anim Genet 38:384–388

Anistoroaei R, Fredholm M, Christensen K, Leeb T (2008) Albinism in the American mink (Neovison vison) is associated with a tyrosinase nonsense mutation. Anim Genet 39:645–648

Anistoroaei R, ten Hallers B, Nefedov M, Christensen K, de Jong P (2011) Construction of an American mink Bacterial Artificial Chromosome (BAC) library and sequencing candidate genes important for the fur industry. BMC Genom 12:354

Anistoroaei R, Krogh AK, Christensen K (2012) A frameshift mutation in the *LYST* gene is responsible for the Aleutian color and the associated Chediak-Higashi syndrome in American mink. Anim Genet 44(2):178–183

Benkel BF, Rouvinen-Watt K, Farid H, Anistoroaei R (2009) Molecular characterization of the Himalayan mink. Mamm Genome 20(4):256–259

Bennett DC, Huszar D, Laipis PJ, Jaenisch R, Jackson IJ (1990) Phenotypic rescue of mutant brown melanocytes by a retrovirus carrying a wild-type tyrosinase-related protein gene. Development 110:471–475

Berryere TG, Schmutz SM, Schimpf RJ, Cowan CM, Potter J (2003) TYRP1 is associated with dun coat colour in Dexter cattle or how now brown cow? Anim Genet 34:169–175

Cirera S, Markakis MN, Christensen K, Anistoroaei R (2013) New insights into the melanophilin (MLPH) gene controlling coat colour phenotypes in American mink. Gene 527(1):48–54

Galante PAF, Sakabe NJ, Kirschbaum-Slager N, de Souza SJ (2004) Detection and evaluation of intron retention events in the human transcriptome. RNA 10:757–765

Graphodatsky A, Yang F, Serdukova N, Perelman P, Zhdanova N, Ferguson-Smith M (2000) Dog chromosome-specific paints reveal evolutionary inter- and intrachromosomal rearrangements in the American mink and human. Cytogenet Cell Genet 90:275–278

Gratten J, Beraldi D, Lowder BV, McRae AF, Visscher PM, Pemberton JM, Slate J (2007) Compelling evidence that a single nucleotide substitution in TYRP1 is responsible for coat-colour polymorphism in a free-living population of Soay sheep. Proc Biol Sci 274:619–626

Halaban R, Moellmann G (1990) Murine and human b locus pigmentation genes encode a glycoprotein (gp75) with catalase activity. Proc Natl Acad Sci USA 87:4809–4813

Hameister H, Klett C, Bruch J, Dixkens C, Christensen K (1997) Zoo-FISH analysis: the American mink (Mustela vison) closely resembles the cat karyotype. Chromosome Res 5(1):5–11

Hearing VJ (1999) Biochemical control of melanogenesis and melanosomal organization. J Invest Dermatol Symp Proc 4:24–28

Hearing VJ (2005) Biogenesis of pigment granules: a sensitive way to regulate melanocyte function. J Dermatol Sci 37:3–14

Hearing VJ, Tsukamoto K (1991) Enzymatic control of pigmentation in mammals. FASEB J 5:2902–2909

Jackson IJ (1988) A cDNA encoding tyrosinase-related protein maps to the brown locus in mouse. Proc Natl Acad Sci USA 85:4392–4396

Kenny EE, Timpson NJ, Sikora M, Yee M-C, Moreno-Estrada A, Eng C, Huntsman S, Burchard EG, Stoneking M, Bustamante CD, Myles S (2012) Melanesian blond hair is caused by an amino acid change in TYRP1. Science 336(6081):554

King RC (1951) Genetics of mink. International Publishers Co, Duluth

Kobayashi T, Hearing VJ (2007) Direct interaction of tyrosinase with Tyrp1 to form heterodimeric complexes in vivo. J Cell Sci. 120(Pt 24):4261–4268

Kobayashi T, Urabe K, Winder A, Jimenez-Cervantes C, Imokawa G, Brewington T, Solano F, Garcia-Borron JC, Hearing VJ (1994) Tyrosinase related protein 1 (TRP1) functions as a DHICA oxidase in melanin biosynthesis. EMBO J 13:5818–5825

Lamoreux LM, Delmas V, Larue L, Bennett DC (2010) The colors of mice. A model genetic network. Wiley, Hoboken. ISBN 978-1-4051-7954-6

Langmead B, Salzberg SL (2012) Fast gapped-read alignment with Bowtie 2. Nat Meth 9(4):357–359

Luo R, Liu B, Xie Y, Li Z, Huang W, Yuan J, He G, Chen Y, Pan Q, Liu Y, Tang J, Wu G, Zhang H, Shi Y, Liu Y, Yu C, Wang B, Lu

Y, Han C, Cheung DW, Yiu SM, Peng S, Xiaoqian Z, Liu G, Liao X, Li Y, Yang H, Wang J, Lam TW, Wang J (2012) SOAPdenovo2: an empirically improved memory-efficient short-read de novo assembler. GigaScience 1:18

Lyons LA, Foe IT, Rah HC, Grahn RA (2005) Chocolate coated cats: TYRP1 mutations for brown color in domestic cats. Mamm Genome 16:356–366

Mohanty TR, Seo KS, Park KM, Choi TJ, Choe HS, Baik DH, Hwang IH (2008) Molecular variation in pigmentation genes contributing to coat colour in native Korean Hanwoo cattle. Anim Genet 39(5):550–553

Nadeau NJ, Mundy NI, Gourichon D, Minvielle F (2007) Association of a single-nucleotide substitution in TYRP1 with roux in Japanese quail (Coturnix japonica). Anim Genet 38:609–613

Nes NN, Einarsson EJ, Lohi O (1988) Beautiful fur animals—and their colour genetics. Scientifur, Hilleroed

Nonneman D, Shibuya H, Johnson GS (1996) A BstUI PCR/RFLP in the bovine tyrosinase-related protein-1 (TYRP1) gene. Anim Genet 27(3):218–219

Ozeki H, Ito S, Wakamatsu K, Hirobe T (1995) Chemical characterization of hair melanins in various coat-color mutants of mice. J Invest Dermatol 105:361–366

Raadsma HW, Jonas E, Fleet MR, Fullard K, Gongora J, Cavanagh CR, Tammen I, Thomson PC (2013) QTL and association analysis for skin and fibre pigmentation in sheep provides evidence of a major causative mutation and epistatic effects. Anim Genet 44(5):547–559

Ren J, Mao H, Zhang Z, Xiao S, Ding N, Huang L (2011) A 6-bp deletion in the TYRP1 gene causes the brown colouration phenotype in Chinese indigenous pigs. Heredity 106:862–868

Rieder S, Taourit S, Mariat D, Langlois B, Guérin G (2001) Mutations in the agouti (ASIP), the extension (MC1R), and the brown (TYRP1) loci and their association to coat color phenotypes in horses (Equus caballus). Mamm Genome 12(6):450–455

Schmidt-Küntzel A, Eizirik E, O'Brien SJ, Menotti-Raymond M (2005) Tyrosinase and tyrosinase related protein 1 alleles specify domestic cat coat color phenotypes of the albino and brown loci. J Hered 96:289–301

Schmutz SM, Berryere TG, Goldfinch AD (2002) TYRP1 and MC1R genotypes and their effects on coat color in dogs. Mamm Genome 13(7):380–387

Shackelford RM (1980) Domestic Production of Mink and Foxes. In: Proceedings of the 29th annual National Breeders' Roundtable. http://www.poultryscience.org/docs/pba/1952-2003/1980/1980%20Shackelford.pdf

Sturm RA, O'Sullivan BJ, Box NF, Smith AG, Smit SE, Puttick ER, Parsons PG, Dunn IS (1995) Chromosomal structure of the human TYRP1 and TYRP2 loci and comparison of the tyrosinase-related protein gene family. Genomics 29(1):24–34

Toyofuku K, Wada I, Valencia JC, Kushimoto T, Ferrans VJ, Hearing VJ (2001) Oculocutaneous albinism types 1 and 3 are ER retention diseases: mutation of tyrosinase or Tyrp1 can affect the processing of both mutant and wild-type proteins. FASEB J 15(12):2149–2161

Walsh PS, Metzger DA, Higuchi R (1991) Chelex 100 as a medium for simple extraction of DNA for PCR-based typing from forensic material. Biotechniques 10:506–513

Wang N, Hebert DN (2006) Tyrosinase maturation through the mammalian secretory pathway: bringing color to life. Pigment Cell Res 19:3–18

Zdarsky E, Favor J, Jackson IJ (1990) The molecular basis of *brown*, an old mouse mutation, and of an induced revertant to wild type. Genetics 126(2):443–449

Zerbino DR, Birney E (2008) VELVET: algorithms for *de novo* short read assembly using de Bruijn graphs. Genome Res 18:821–829

Zhang Z, Xin D, Wang P, Zhou L, Hu L, Kong X, Hurst LD (2009) Noisy splicing, more than expression regulation, explains why some exons are subject to nonsense-mediated mRNA decay. BMC Biol 7:23